Research and Development of a Lateral Stress Piezocone

R. G. CAMPANELLA, J. P. SULLY, J. W. GREIG, AND G. JOLLY

The possibility of evaluating in situ horizontal stress during cone penetration has been suggested by recent laboratory calibration chamber research (*1–6*). This has been confirmed by field trials with lateral stress sensing cones. A lateral stress piezocone developed at the University of British Columbia is described. Detail is given of the laboratory calibration procedures and corrections for cross talk and temperature effects. Field data from two Lower Mainland sites are presented to evaluate the amplification of lateral stress that occurs in sands during penetration of full-displacement probes. The results suggest that lateral stresses measured in granular soils with the LS cone are dependent on, *inter alia*, the existing horizontal stress, in situ state of the sand, and its grain characteristics.

Recent research into the behavior of granular soils during cone penetration has highlighted the importance of the existing in situ horizontal effective stress (σ_h') on the parameters being measured. Laboratory measurements made by using calibration chambers (CC) have demonstrated the effects of in situ stress state on both cone resistance and sleeve friction (*7*). Similar effects noted for other penetration parameters are consistent with those findings.

The development of cones capable of measuring lateral stress originated from the idea that the sleeve friction measured during penetration in sand should be related to the pre-penetration lateral stress. Robertson (*6*) evaluated the CC data for sand presented by Baldi et al. (*7*) and showed that the ratio of pre- and post-penetration horizontal stress, as was deduced from sleeve friction measurements, varied from 1 to 7 and was related to the maximum dilation angle of the soil. The data were obtained for the friction sleeve located directly behind the tip. The CC tests were performed under conditions of constant lateral stress (BC1).

Huntsman (*2*) reviewed similar CC data from Italy and related σ_h' and sleeve friction f_s by means of the relative density D_r of the sand. Two sets of data were presented corresponding to the boundary conditions of constant lateral stress (BC1) and zero lateral strain (BC3). The scatter in the results is appreciable. However, the data trends do illustrate the effect of boundary condition on the σ_h'-f_s correlation (Figure 1) and indicate that at low relative densities the measured sleeve friction is less sensitive to the applied boundary condition. The true correlation representing "in-ground" conditions probably lies somewhere between the two data sets in Figure 1 and can be estimated by applying the appropriate chamber corrections.

R. G. Campanella, J. P. Sully, and J. W. Greig, Department of Civil Engineering, University of British Columbia, Vancouver, B.C. V6T 1W5 Canada. G. Jolly, Adara Systems Ltd., 2443 Beta Avenue, Burnaby, British Columbia, V5C 5N1, Canada.

On the basis of those findings, several types of cone penetrometer have been produced that are capable of measuring the lateral stress that act on an under-reamed section of a friction sleeve: (a) lateral stress sensing cone penetrometer (*2*) and (b) horizontal stress cone (*4*). A similar type of instrument designed specifically for evaluation of pile capacity in cohesive soils—the piezo-lateral stress cell—has been built and tested at MIT (*8*).

This paper describes a lateral stress (LS) piezocone designed and built at the University of British Columbia (UBC) for use as part of a research project that will evaluate in situ lateral stress from full displacement probes.

DETAILS OF LATERAL STRESS PIEZOCONE

The LS piezocone designed and built at UBC comprises two separate measurement systems: a standard UBC piezocone unit followed by a LS module. The eight-channel cone has a tip area of 15 cm^2, a friction sleeve area of 225 cm^2, and allows the simultaneous measurement of the following parameters:

- Cone resistance, q_c (bar);
- Pore pressure on the face, u_1, or behind the tip, u_2 (m of water);
- Sleeve friction, f_s (bar);
- Pore pressure behind the friction sleeve, u_3 (m of water); and
- Temperature (°C).

Those channels operate over a 7.5-V range. The calibration factors for each channel are given in Table 1. The LS module, which essentially consists of an instrumented friction sleeve, is located 0.69 m behind the tip and permits the following values to be recorded:

- Sleeve friction, LS-FS (bar);
- Pore pressure, u_{LS} (m of water);
- Lateral stress, σ_{LS} (kPa); and
- Temperature (°C).

Even though two temperature sensors are located in the LS-CPTU, only the temperature at the lateral stress module position is recorded when the cone is being used in this format.

The transducer ranges are again 7.5 V for all the channels except the lateral stress channel, which operates on 1 V full scale. The choice of location for the lateral stress module requires some comment.

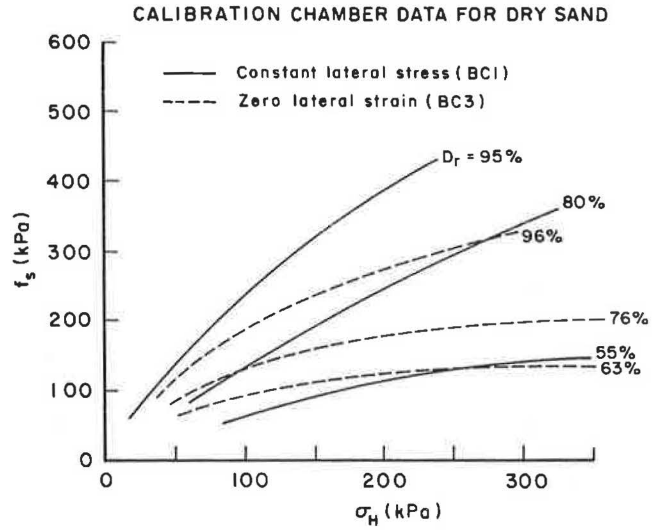

FIGURE 1 Influence of relative density on $f_s - \sigma_h'$ relationship from CC test data [after Huntsman (2)].

Design Considerations

Studies into soil behavior have demonstrated that large gradients of both stress and pore pressure exist around a penetrating cone and that those gradients are related primarily to the geometry of the equipment. In effect, the singularity at the base of the cone tip causes a large normal stress reduction to occur as the soil passes the shoulder. The extent of the reduction has been experimentally evaluated with respect to pore pressures (9), but little information exists with respect to lateral stress reduction and the relative importance of stress redistribution and creep. Indirect evidence for sands based on the variation of average sleeve friction, f_s, with distance (10) suggests that at approximately 12*D* (*D* = diameter of cone) behind the tip the lateral stress should be essentially constant for any particular D_r.

Location of the lateral stress sensor close to the tip would require measurement in an area of highly variable stress. Furthermore, at this location, dimensional tolerances may have unacceptable effects on the measured values (i.e., a slightly undersized friction sleeve may promote a larger stress reduction whereas an oversized sleeve may reduce the unloading effect). Strain rate changes near the tip and rotation of principal stresses may also be important. This aside, both Huntsman (2) and Jefferies et al. (4) present data where the lateral stress measured during cone penetration by a sensor located 1*D* behind the tip corresponds remarkably well to results of self-bored pressuremeter tests. This is surprising, considering the disturbance caused by insertion of the cone, and may well result from the loose nature of the soils tested. When penetration is stopped, however, the tests performed by Huntsman in the Beaufort Sea (2) indicated a slight increase in measured total lateral stress with time. That increase may result from redistribution and dissipation or both of excess pore pressures generated during penetration. However, no pore pressure measurements are available to confirm this.

The location of the sensor close to the tip is advantageous where reference tests are performed in calibration chambers. Calibration of an upper stress sleeve is not possible owing to the limited penetration distance that results from chamber size. CC data suggest that the measured lateral stress is always lower when measured close to the tip. Field data from the Beaufort Sea indicate that the difference between the stresses measured behind the tip (1*D*) and up the shaft (8*D*) decreases with depth, becoming equal at approximately 20 m (2). However, the relative magnitudes of σ_{LS} would depend on the location and spacing of the lateral stress sensors.

No CC facility exists at UBC, and, consequently, it was planned to calibrate the LS cone initially in the laboratory and then in the field at sites where the K_o condition was approximately known. As such, the geometry of the cone in terms of sensor location was not a restriction.

Finally, with a view to developing some kind of theoretical interpretation, it is reasonable to expect that data obtained away from the tip may more closely represent conditions of cylindrical cavity expansion. Stress changes near the tip may cause significant deviation from the cavity expansion condition.

Details of LS Module

For the UBC LS piezocone, the sensor is located 0.69 m (15.6*D*) behind the cone shoulder (Figure 2). The LS sleeve is 88 mm long and 44 mm in diameter (surface area of 121.6 cm^2) with a wall thickness of 3 mm. At the center of the sleeve, a 20-mm-long section has a reduced wall thickness of 1 mm. An arrangement of strain gauges is oriented at this location to measure the hoop stress in the section induced by the lateral stress acting on the sleeve. Several different gauge

TABLE 1 CALIBRATION DATA FOR LS PIEZOCONE

Channel No.	Parameter	Units	Calibration Factor
1	Cone resistance	bar	0.13 bar/mV
2	Sleeve friction	bar	0.013 bar/mV
3	Lower pore pressure	m of water	0.23 kPa/mV
4	Upper pore pressure	m of water	0.23 kPa/mV
5	Temperature	degree C	*
6	LS-FS	bar	0.013 bar/mV
7	LS-PP	m of water	0.23 kPa/mV
8	σ_{LS}	kPa	1.44 kPa/mV

* Temperature in degrees Celsius is obtained from $(V_T x4)-11$ where V_T is the voltage measured from a resistance temperature device (RTD).

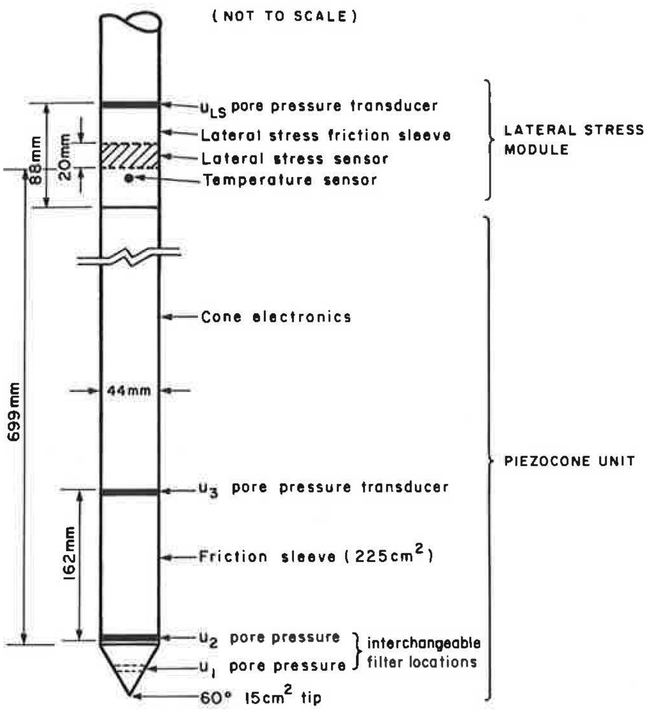

FIGURE 2 LS cone details.

arrangements were tested to optimize the lateral stress response and minimize both temperature and friction cross-talk effects.

A full bridge configuration is mounted on the sleeve. Each arm of the bridge consists of two 1,000 ohm strain gauges. The active arms are located on the thin-walled section of the sleeve, and the inactive arms are on the thicker section. The current design remains temperature sensitive to some degree, and, consequently, a platinum RTD sensor has been installed in the sleeve to allow for temperature compensation corrections to both the LS and the sleeve friction measurements.

The differential signals from the LS gauges are amplified in the cone to give a full-scale output of 1 V for an external hydrostatic pressure of approximately 1,500 kPa. The analog signals are converted at the surface to a 12-bit representation of the voltage, giving a sensitivity of 4.9 mV or 7.4 kPa of lateral stress. The IBM PC-based data acquisition system (UBC DAS) consists of an analog-to-digital (A/D) converter, depth controller board, counter timer board, and a battery backed-up power supply (*11*). A schematic layout of the UBC DAS is presented in Figure 3.

The data acquisition program interfaces the various components of the system to provide a means of collecting and storing the data. Data storage is either on floppy or hard disk. The program operates in two modes: cone penetration and dissipation. The change to dissipation mode is automatic when penetration is halted.

LABORATORY CALIBRATION OF LSC

Laboratory calibration of the load cells and pore pressure transducers for the piezocone unit were performed according to standard procedures adopted at UBC. Only the laboratory calibration of the lateral stress module is considered here.

Owing to the nature of the design of the module, it was necessary to calibrate the module for the following conditions:

- Hydrostatically applied confining pressure,
- LS cross talk on friction sleeve owing to axial loads,
- Temperature sensitivity, and
- Time-dependent stability of all channels.

During each of the calibrations performed, all eight cone channels were monitored to ensure the absence of channel interference.

Hydrostatic Calibration of LS Module

A special sleeve was fitted over the LS module and connected to a dead weight pressure tester to calibrate the bridge output for applied hydrostatic pressure. Pressure increments of 20 psi (~138 kPa) were used, up to a maximum of 250 psi (1724 kPa), and a constant temperature was maintained throughout. Hydrostatic loading and unloading sequences were performed for conditions of zero axial load. The results are presented in Figure 4 that give a calibration factor of 0.000695 V/kPa or 1440 kPa/V, with little or no hysteresis effects and no baseline drift over full-scale cycling. The factor was independent of temperature for the range of application (6° to 20°C).

FRICTION-LS CROSS TALK

Axial loading of the friction sleeve causes an output voltage on the LS channel because of the Poisson effect. Increasing sleeve friction on the LS sleeve for the strain gauge arrangement employed causes a negative offset on the LS channel.

The cone was set up in a frame so that the axially applied load was transferred by slip rings to the LS friction sleeve. Data from both the LS and the sleeve friction channels were recorded by an HP7090A measurement-plotting system. The load-unload was performed under zero confining pressure over a period of approximately 1 min, with readings taken every 0.1 sec. Linear regression of the data gave gradients of −0.2136 and −0.2150 for loading and unloading (Figure 5). A correction factor of 0.807 is applied to the slope in Figure 5, which takes into account the difference between the axial load distribution imposed for the laboratory calibration and actual field conditions.

An average value was used to correct the lateral stress data according to the equation

$$(V_{LS})_C = (V_{LS})_M + (0.2143 \times V_{fs}) \quad (1)$$

where

$(V_{LS})_C$ = corrected relative LS voltage,
$(V_{LS})_M$ = measured relative LS voltage, and
V_{fs} = relative sleeve friction voltage.

Calibration for Temperature Effects

To evaluate the temperature sensitivity of the LS module, the whole cone was immersed in a bath of ice water and was left

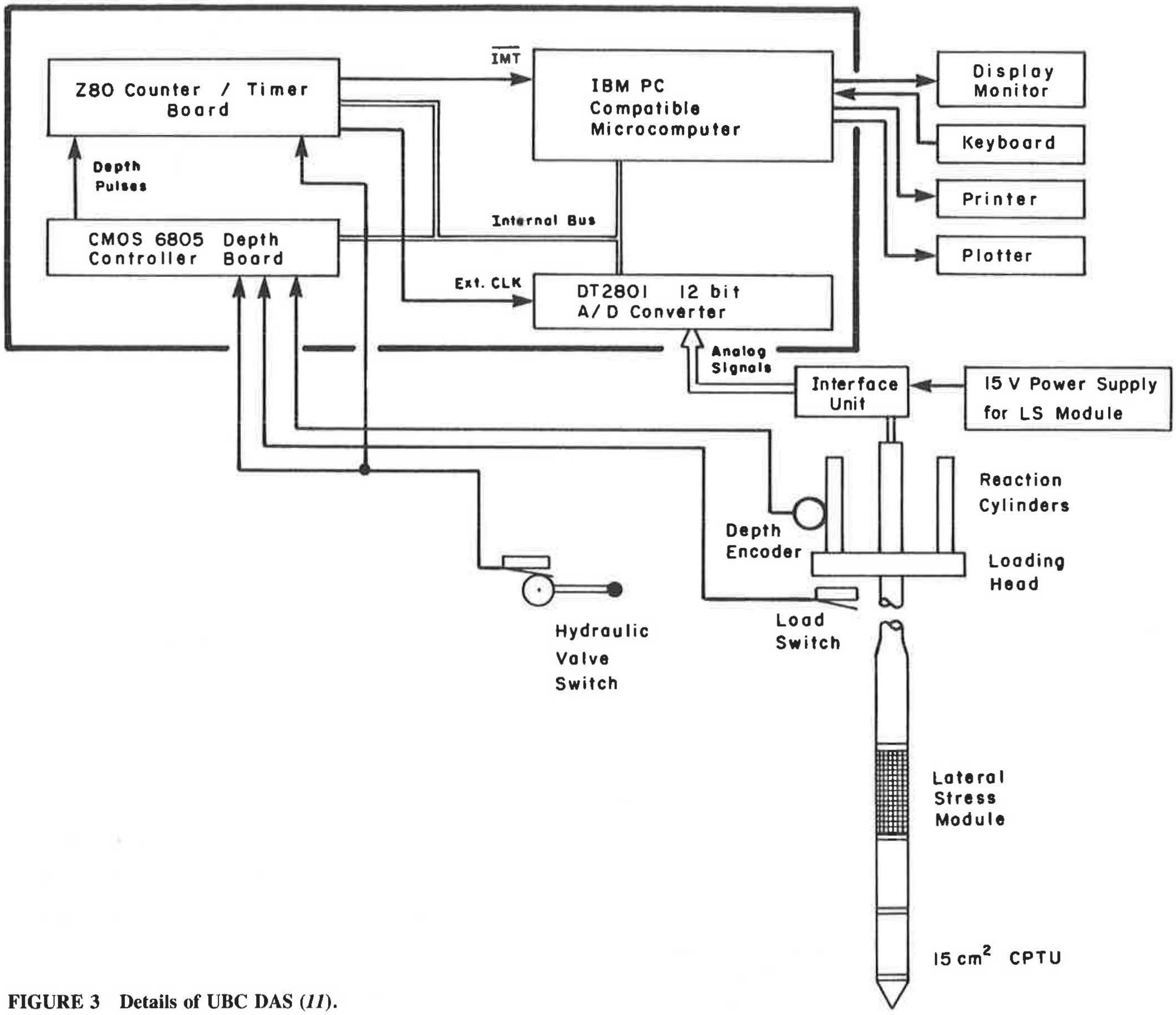

FIGURE 3 Details of UBC DAS (*11*).

to warm to room temperature over a 24-hr period, during which time readings on all channels were taken every minute. The results for the LS channel are presented in Figure 6. The temperature coefficient B_T for the LS channel was calculated to be +3.6 mV/°C on cooling. (Similarly, temperature coefficients were also evaluated for other channels.)

Evaluation of Baseline Drift

During the latter part of the temperature calibration, when the system was in equilibrium with the ambient temperature, continued monitoring allowed baseline drift on each channel to be evaluated. The time-dependent drift was found to be negligible for all eight channels.

The calibration factors obtained as just outlined have been incorporated into the data-acquisition program so that the output is given in corrected engineering units.

FIELD CALIBRATION OF LS PIEZOCONE

As was mentioned, field calibration of the LS cone equipment were performed at UBC test sites where information on LS conditions was available. For the purpose of this paper, only tests in granular soils are considered. Data obtained in cohesive soils are presented in a companion paper to this symposium (*12*).

The LS measured during cone penetration is generally larger than the pre-penetration in situ horizontal stress and results from the full-displacement mode of insertion where soil is displaced both laterally and vertically to permit penetration of the cone. Consequently, an overall stress increase around the penetrating cone usually occurs, and it is this value measured by the instrumented sleeve. The magnitude of the measured stress increase depends on the location of the sensor, geometry of the probe, and soil characteristics. For a partic-

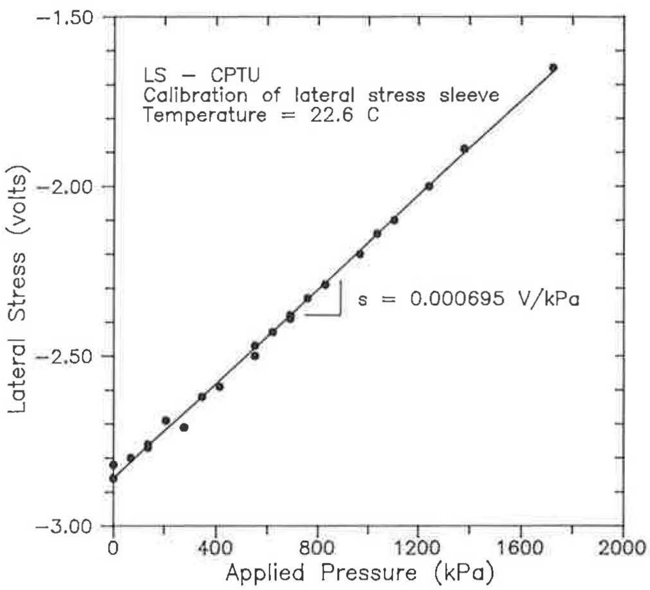

FIGURE 4 Pressure calibration of LS module.

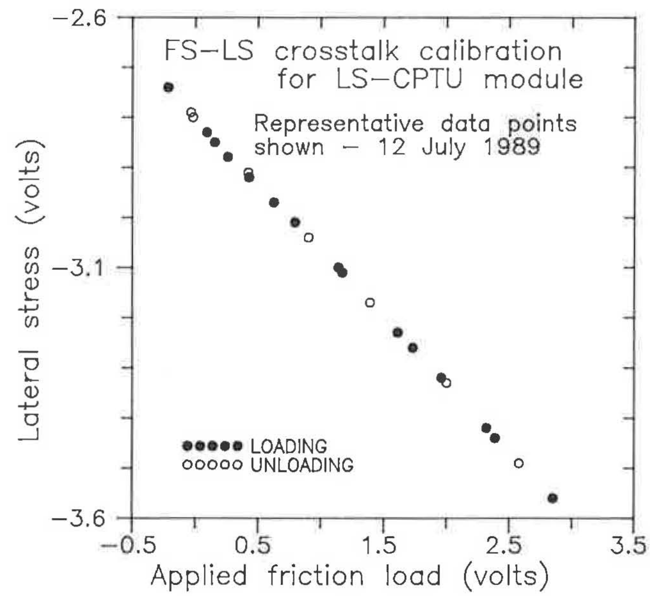

FIGURE 5 Evaluation of cross talk on LS channel owing to axial friction load.

ular probe the stress increase can thus be related to one or more soil parameters.

Studies have suggested that the stress increment caused by full-displacement penetration in granular soils is a function of one or more of the following points:

- Relative density of the soil, D_r (*2*);
- Peak friction angle, ϕ, or maximum angle of dilation, μ (*6*);
- Voids ratio, e (*4*); and
- State parameter, ψ (*2,4*).

The state parameter/voids ratio approach has been used primarily for evaluating CC data where sample characteristics can be controlled and measured with acceptable accuracy (*4*). The application of the state parameter approach to in situ data appears promising but requires further confirmation. As was suggested by Sladen (*13*), the approach may necessitate additional specialized in situ tests to confirm the void ratios evaluated on the basis of CPT data (i.e., nuclear density/electrical resistivity voids ratio determinations) and also requires, a priori, knowledge of the in situ LS.

A considerable data base exists for estimating both relative density and peak friction angle from CPT data. The use of either one of those parameters would also concur with the philosophy of field calibration. Alternatively, correlation with the ratio q_c/σ'_v would appear logical as the dependence on a CC-derived relationship is removed.

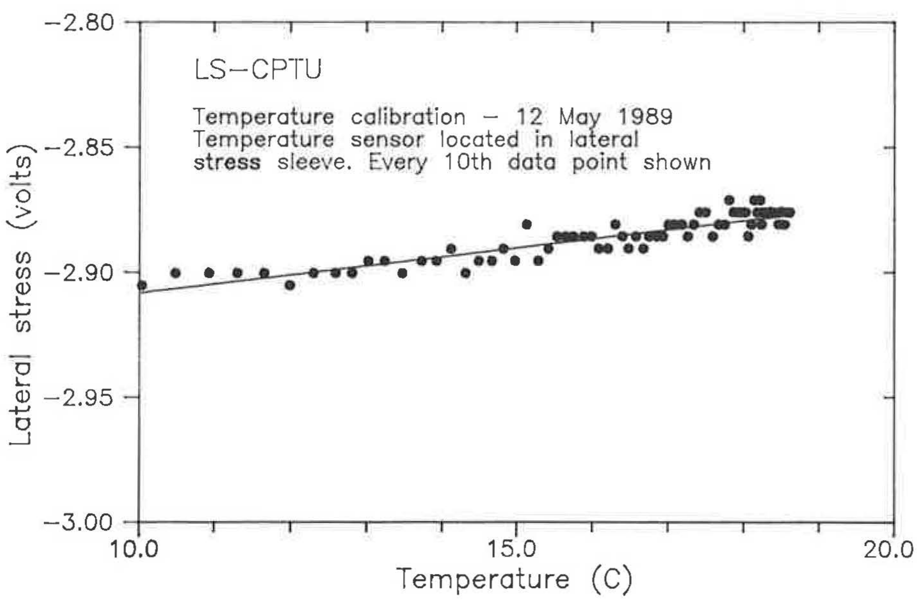

FIGURE 6 Temperature sensitivity of LS baseline.

Description of Test Sites

Data from two UBC test sites in the Lower Mainland of British Columbia are presented where consistent information on K_o conditions exists: Laing Bridge South (LBS) and McDonald Farm (MDF). The two sites are located on Sea Island at Vancouver International Airport, are about 1 km apart, and have very similar characteristics. The sediments are post-glacial Holocene deltaic deposits, which are essentially normally consolidated. The surficial soils (<4 m) are underlain by granular marine and tidal flat deposits (medium sands) to a depth of around 20 m. The granular layer is finer grained, more uniform, and deeper at LBS than at MDF. Underlying the sands are at least 40 m of soft-to-firm marine silts and clayey silts.

The variation of K_o for the LBS site is presented in Figure 7 and has been evaluated by three empirical correlations (*14*). The K_o value varies between 0.45 and 0.5. Preliminary results obtained by using the UBC self-boring pressuremeter confirm the K_o values in Figure 7.

Data presented by Hughes and Robertson (*15*) from self-bored pressuremeter tests suggest that the LBS trend of K_o is a good lower bound for the MDF site, where an average coefficient of 0.6 is taken as representative for the normally consolidated sands.

RESULTS OF IN SITU TESTS

A summary of the measured cone resistance and lateral stress profiles for MDF and LBS are presented in Figures 8 and 9.

Considering the proximity of the sites, the trends in q_c at the two sites are notably different. At MDF the q_c values are reasonably constant over specific depth intervals within the sand. The gradual increase in q_c with depth at LBS is a good indicator of the uniformity of the sand at this location. The effects of interbedded silt on the cone resistance at both sites can be seen throughout the profile. Pore pressures throughout the profile are close to hydrostatic for both the behind friction sleeve (u_3) and the lateral stress (u_{LS}) pore pressure sensor locations. A small excess pore pressure is measured behind the tip (u_2). At around 14 m, the anomalously high q_c results from the presence of an organically cemented sand layer, a remnant of an active beach deposit. At the base of the sand layer the q_c values drop rapidly to around 10 bar, and large excess pore pressures are recorded that indicate the presence of the soft normally consolidated clay silt.

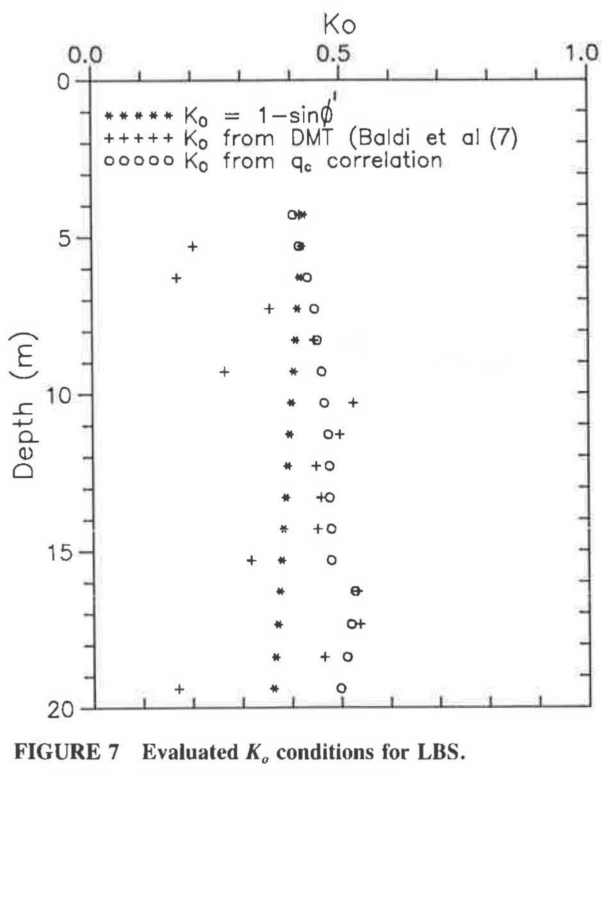

FIGURE 7 Evaluated K_o conditions for LBS.

The lateral stress profiles measured by the LS cone at the two sites are also presented in Figures 8 and 9. Contrary to the relative magnitudes of cone resistance, the measured total LS σ_{LS} in the sand layer at LBS is consistently larger than that at MDF. The σ_{LS} profiles are otherwise very similar. The variation in measured σ_{LS} at both sites is increased in the transition layer between the sand and clay silt.

A comparison of average friction stress measured at the two sleeve locations is presented in Figure 10 for LBS. Good agreement between the two measurements is evident and concurs with the distribution suggested earlier by Campanella and Robertson (*10*). This also suggests that the LS measurements at the 15.6*D* position might be similar to those at the 1*D* location previously investigated. However, this conclusion would depend on the stress gradient behind the tip and the exact location of the LS sensing section in relation to the stress distribution.

The penetration pore pressures measured at the three sensor locations, (i.e., behind tip, behind friction sleeve, and at LS sleeve), are presented in Figure 11 for the MDF LS-CPTU. The similarity of the pore pressures measured behind the friction sleeve (u_3) and at the LS section (u_{LS}) indicate the absence of large gradients once away from the tip-shoulder singularity. Also apparent when comparing Figures 8 and 11 is that the measured LS in fine-grained materials is dominated by the pore pressure response.

LS Coefficient from LS-CPTU

The LS coefficient obtained from LS-CPTU profiling K_{LS} is defined as

$$K_{LS} = \frac{\sigma_{LS} - u_{LS}}{\sigma'_v} \qquad (2)$$

where

σ_{LS} = measured total LS,
u_{LS} = penetration pore pressure measured at LS section, and
σ'_v = calculated effective overburden pressure.

Statistical filtering of calculated K_{LS} values at 2.5-cm intervals was performed over a 25-cm window. All data outside 1 standard deviation of the median were removed and replaced by the mean value (*16*). The filtered profiles of K_{LS} for both sites are presented in Figure 12, where it can be seen that, in

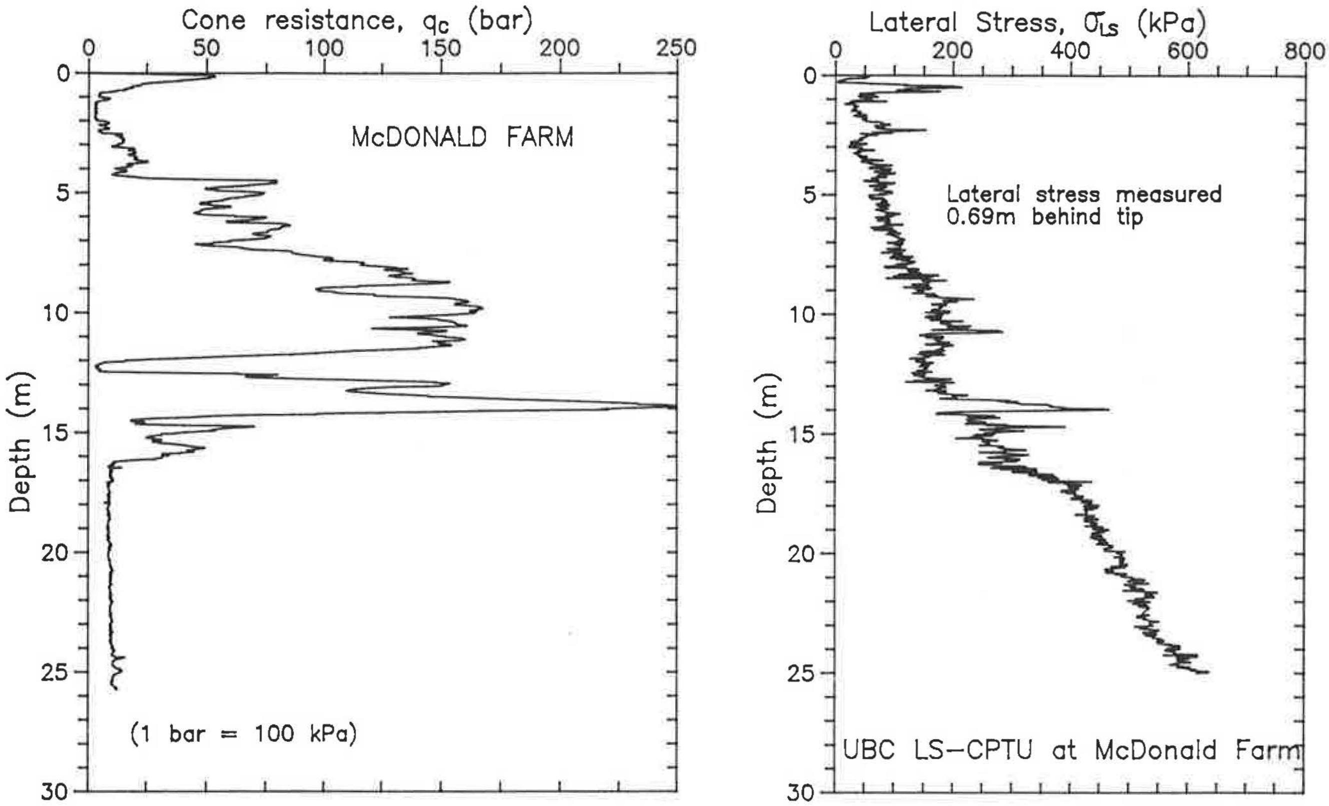

FIGURE 8 LS-CPTU results at MDF.

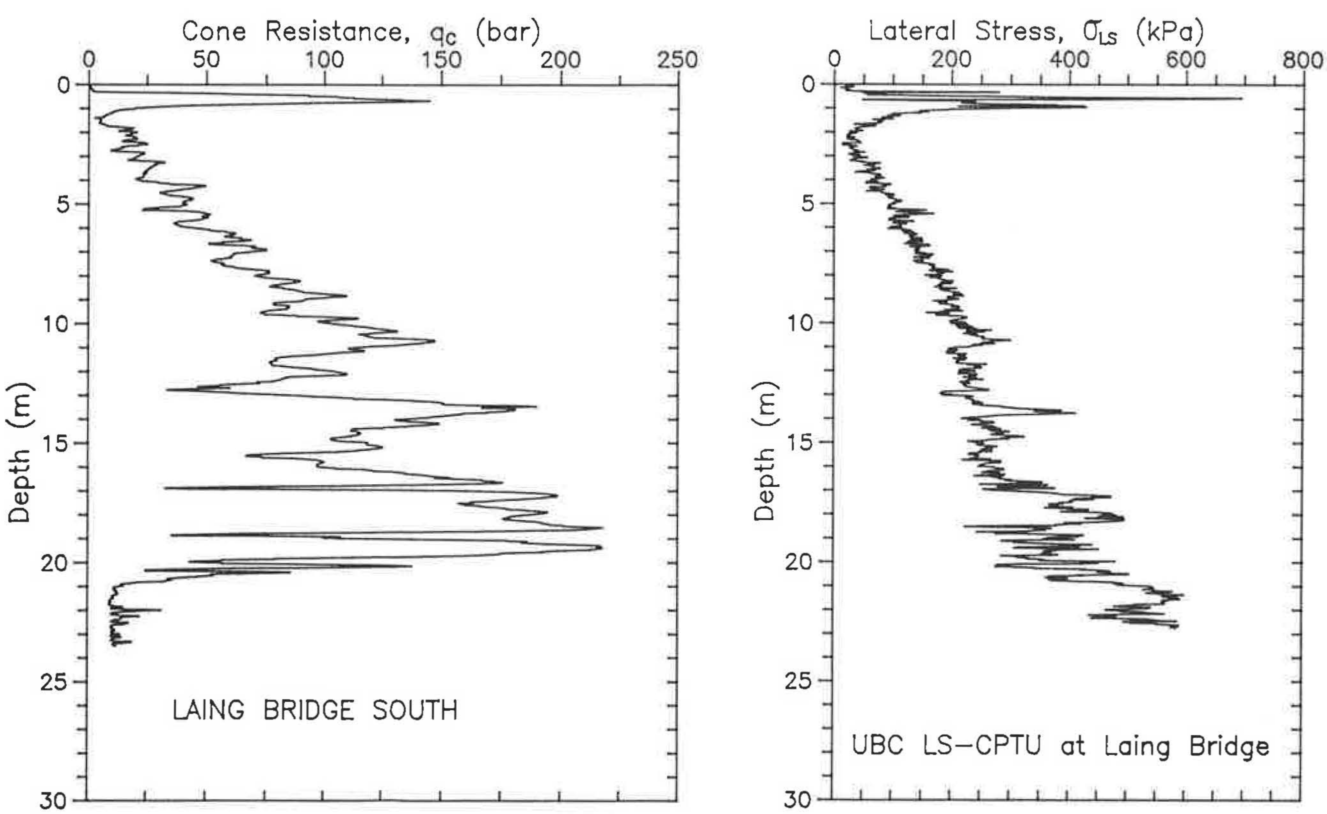

FIGURE 9 LS-CPTU results at LBS.

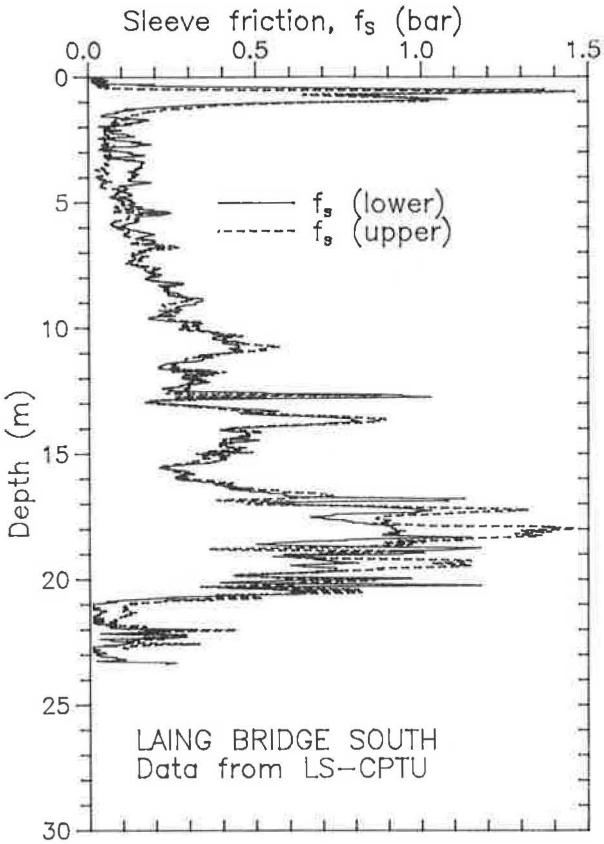

FIGURE 10 Comparison of average sleeve friction measured at two locations on LS cone.

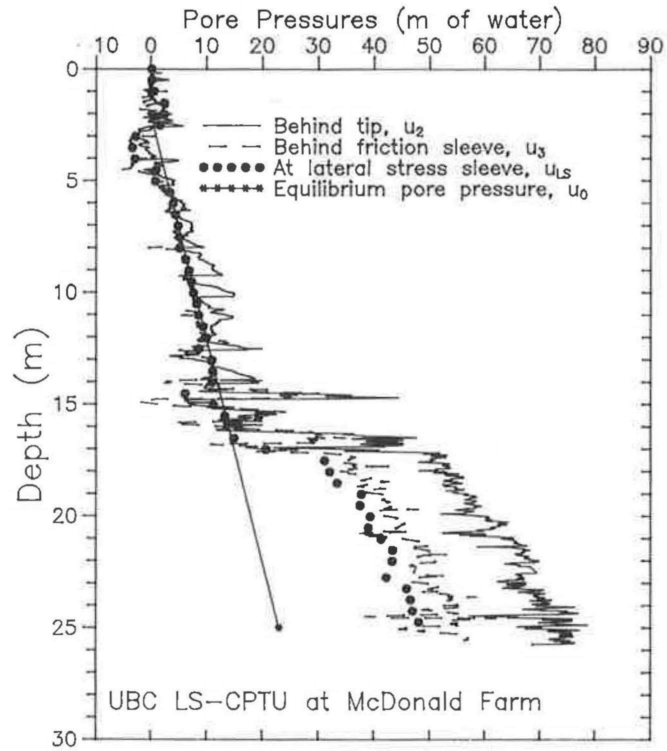

FIGURE 11 Pore pressures measured during LS-CPTU.

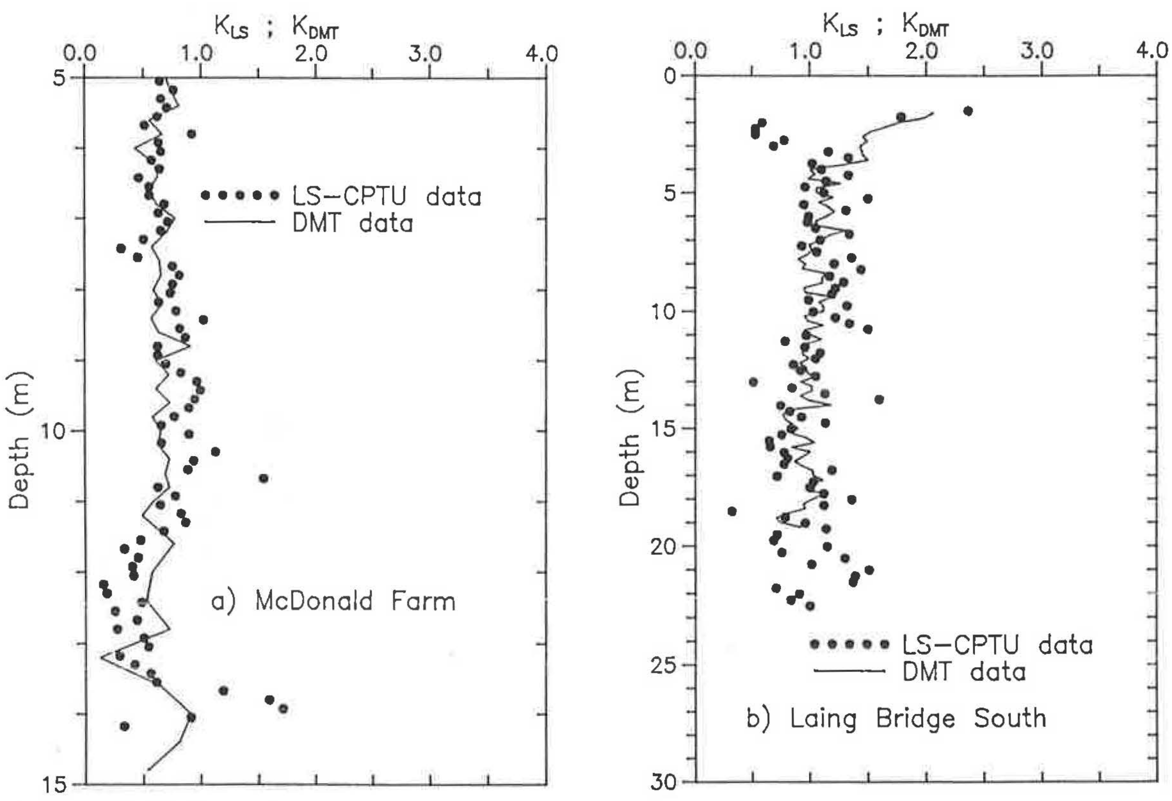

FIGURE 12 K_{LS} factors for test sites.

general, $K_{LS} > K_o$. To evaluate the amplification of LS caused by cone penetration, the effective LS in Figure 12 has been normalized with respect to the in situ σ'_h and replotted in Figure 13 against q_c/σ'_v. The amplification factor for the LS cone A_{LS} is defined as

$$A_{LS} = \frac{\sigma'_{LS}}{\sigma'_h} = \frac{\sigma_{LS} - u_{LS}}{\sigma_h - u_0} \tag{3}$$

where σ'_h is the prepenetration effective horizontal stress and u_0 is the equilibrium in situ pore pressure. By definition

$$K_o = \frac{K_{LS}}{A_{LS}} \tag{4}$$

The basis of obtaining σ'_h was discussed earlier. Use of q_c/σ'_v as an index parameter appears logical because it is related to the principal soil behavior characteristics thought to control the stress amplification effect (*2,4,6*). Furthermore, q_c is a parameter measured during the LS-CPTU and correlates directly with the σ_{LS} values measured (i.e., at the same location).

Two effects are apparent from the trends shown in Figure 13:

1. The amplification factor A_{LS} is very sensitive to small changes in q_c/σ'_v ratio.
2. The shape of the $A_{LS} - q_c/\sigma'_v$ relationship appears to be similar for the two sites studied. However, the curves are offset laterally owing to some secondary effect.

The position of a tentative curve for data obtained in silt/silty sand is also shown and further suggests that grain size characteristics (D_{50}, silt content, grain angularity) of the sand may be important factors when evaluating LS amplification factors in the manner used here.

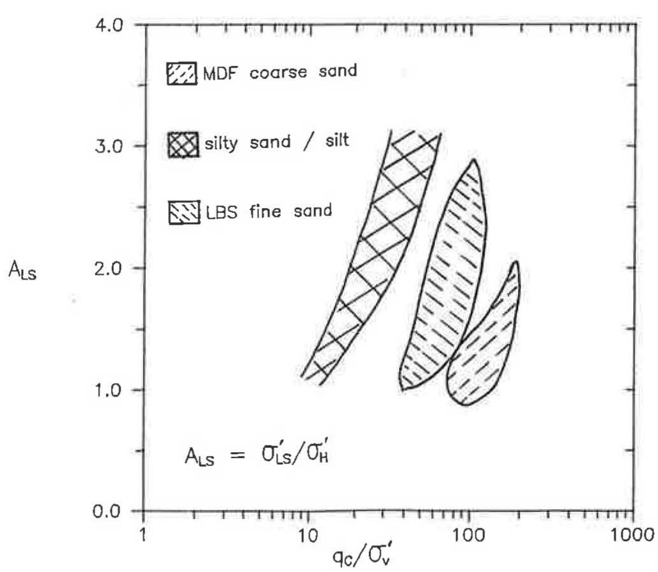

FIGURE 13 Lateral stress amplification factor for soils tested.

DISCUSSION

The results obtained in this study agree with other data trends obtained from calibration chamber tests and interpreted to evaluate LS from full-displacement tests (*1,3,5,6*). In clays, the LS cone response is dominated by pore pressure effects.

It is interesting to note that LS coefficients obtained from the DMTs performed at MDF and LBS, interpreted by using Schmertmann's method (*17*) to give an estimate of in situ K_o, give the same relative magnitudes as those obtained from direct measurements during LS-CPTU profiling (Figure 12). In general terms,

For MDF

$$K_{LS} \approx K_{DMT} = 1\text{–}1.2\ (K_o) \tag{5}$$

for LBS

$$K_{LS} \approx K_{DMT} = 1.5\text{–}2.5\ (K_o) \tag{6}$$

where K_{DMT} is the K_o value obtained from the interpreted DMT profile (*17*).

The DMT soil type index I_D also suggests that the LBS sand is finer than the MDF sand, as indicated in Figure 13.

Measurement of both friction and normal stress at the upper sleeve location permits an evaluation of the average mobilized soil to steel friction angle during penetration. Friction angles varying between 18 and 25 degrees were obtained for the sand layer at MDF. Lower values were measured for LBS. Tomlinson (*18*) suggests from his experience with steel piles in sand that a soil-steel friction angle of 20 degrees is appropriate. The data are also in agreement with results suggested by a literature review of measured soil-steel friction coefficients and with measurements in ring shear tests performed at UBC (*19*). This would suggest that the relative values of the parameters being measured during LS-CPTU profiling are realistic.

SUMMARY AND CONCLUSIONS

Data have been presented from laboratory and field measurement by using a LS piezocone. Laboratory calibrations have shown that the measured LS is sensitive to both axial loads on the friction sleeve and on temperature. However, those effects can be calibrated out by making corrections to the measured data. The corrections applied are stable and repeatable.

Field measurements suggest that the LS measured by the LS cone is greater than the in situ horizontal stress. The increase over and above the in situ condition in sand has been shown to be partly a function of the normalized cone resistance q_c/σ'_v. It would also appear that grain size, grain size distribution, and angularity may be important.

The measured LS undergoes some degree of dissipation during stops in the penetration of the cone. The reduction in LS appears to be controlled by the characteristics of the soil at the tip and at the sleeve location. Further work is being done to evaluate those effects. Additional studies are presently being performed to evaluate the application of LS cone data to the interpretation of in situ horizontal stress. Refined signal processing will allow the present ±7 kPa resolution on the LS channel to be considerably improved. Variations in the mechanical design of the LS module are also underway.

ACKNOWLEDGMENTS

Financial assistance for the design and construction of the lateral stress module was provided by NSERC as part of a University-Industry Cooperative grant. The second author was supported by an SERK (U.K.) NATO scholarship during this study and which is gratefully acknowledged. The assistance of members of the Civil Engineering Department at UBC is gratefully appreciated. S. Jackson and H. Schrempp are thanked for their assistance in the development of the lateral stress cone.

REFERENCES

1. K. Been, J. H. A. Crooks, and L. Rothenburg. A Critical Appraisal of CPT Calibration Chamber Tests. *Proc., Penetration Testing 1988, ISOPT-1*, Florida, Vol. 2, 1988, pp. 651–660.
2. S. R. Huntsman. *Determination of In Situ Lateral Pressure of Cohesionless Soils by Static Cone Penetrometer*. Ph.D. thesis, University of California, Berkeley, 1985.
3. M. G. Jefferies. Verification of the q_c-ψ Function in Sand Strata. *Proc., Penetration Testing 1988, ISOPT-1*, Florida, Vol. 1, 1988, pp. 793–804.
4. M. G. Jefferies, L. Jönsson, and K. Been. Experience With Measurement of Horizontal Geostatic Stress in Sand During Cone Penetration Test Profiling. *Geotechnique*, Vol. 37, 1987, pp. 483–498.
5. S. Marchetti. On the Field Determination of K_o in Sand. Panel discussion to Session 4A. *Proc., 11th ICSMFE*, San Francisco, Calif., Vol. 4, 1985.
6. P. K. Robertson. *In Situ Testing of Soil With Emphasis on Its Application to Liquefaction Assessment*. Ph.D. thesis, University of British Columbia, Vancov
7. G. Baldi, R. Bellotti, V. (Pasqualini. Design Parameters for Sands From CPT. *Proc., ESOPT II*, Amsterdam, Vol. 2, 1982, pp. 425–438.
8. M. M. Baligh, R. T. Martin, A. S. Azzouz, and M. J. Morrison. The Piezo-Lateral Stress Cell. *Proc., 11th International Conference on Soil Mechanics and Foundation Engineering*, San Francisco, Calif., Aug. 1985, pp. 841–844.
9. D. G. Gillespie. *Evaluating Velocity and Pore Pressure Data From the Cone Penetration Test*. Ph.D. thesis, University of British Columbia, Vancouver, in preparation, 1990.
10. R. G. Campanella and P. K. Robertson. Applied Cone Research. Presented at Symposium on Cone Penetration Testing and Experience, Geotechnical Engineering Division, ASCE, Oct. 1981.
11. J. W. Greig, P. K. Robertson, and R. G. Campanella. Microcomputer Software to Collect, Plot, and Interpret Cone Penetration Test Data. *Proc., 1st Canadian Symposium on Microcomputer Applications to Geotechnics*, Oct. 1987, pp. 75–83.
12. J. P. Sully and R. G. Campanella. Measurement of Lateral Stress in Cohesive Soils by Full-Displacement In Situ Test Methods. *TRB*, this issue.
13. J. A. Sladen. Problems with Interpretation of Sand State From Cone Penetration Test. *Geotechnique*, Vol. 39, 1989, pp. 323–332.
14. J. P. Sully and R. G. Campanella. Correlation of Maximum Shear Modulus With DMT Test Results in Sand. *Proc., 12th ICSMFE*, Rio de Janeiro, Aug. 1989.
15. J. M. O. Hughes and P. K. Robertson. *Full Displacement Pressuremeter Testing in Sand*. Soil Mechanics Series 78. Department of Civil Engineering, University of British Columbia, Vancouver, April 1984.
16. D. S. Wickremesinghe. *Statistical Characterization of Soil Profiles Using In Situ Tests*. Ph.D. thesis, University of British Columbia, Vancouver, June 1989.
17. J. H. Schmertmann. Revised Procedure for Calculating K_o and OCR from DMTs With $I_D > 1.2$ and Which Incorporates the Penetration Force Measurement to Permit Calculating the Plane Strain Friction Angle. Presented at DMT Workshop, March 16–18, Gainesville, Fla., 1983.
18. M. J. Tomlinson. *Pile Design and Construction Practice*. Cement and Concrete Association, London, 1981.
19. N. F. Rinne. *Evaluation of Interface Friction Between Cohesionless Soil and Common Construction Materials*. M.A.Sc. thesis, University of British Columbia, Vancouver, 1989.

aper sponsored by Committee on Soil and Rock